Medical Physics
The International Journal of Medical Physics Research and Practice

Output calculation of electron therapy at extended SSD using an improved LBR method

Hassaan A. Alkhatib, Wondesen T. Gebreamlak, David J. Tedeschi, Dimitris Mihailidis, Ben W. Wright, William J. Neglia, Philip T. Sobash, and Jonas D. Fontenot

Citation: Medical Physics **42**, 735 (2015); doi: 10.1118/1.4905375
View online: http://dx.doi.org/10.1118/1.4905375
View Table of Contents: http://scitation.aip.org/content/aapm/journal/medphys/42/2?ver=pdfcov
Published by the American Association of Physicists in Medicine

Output calculation of electron therapy at extended SSD using an improved LBR method

Hassaan A. Alkhatib and Wondesen T. Gebreamlak[a)]
South Carolina Oncology Associates, Columbia, South Carolina 29210

David J. Tedeschi
Department of Physics and Astronomy, University of South Carolina, Columbia, South Carolina 29208

Dimitris Mihailidis
CAMC Cancer Center and Alliance Oncology, Charleston, West Virginia 25304

Ben W. Wright and William J. Neglia
South Carolina Oncology Associates, Columbia, South Carolina 29210

Philip T. Sobash
The Medical University of South Carolina, Charleston, South Carolina 29425

Jonas D. Fontenot
Department of Physics, Mary Bird Perkins Cancer Center, Baton Rouge, Louisiana 70809

(Received 26 August 2014; revised 31 October 2014; accepted for publication 19 December 2014; published 14 January 2015)

Purpose: To calculate the output factor (OPF) of any irregularly shaped electron beam at extended SSD.
Methods: Circular cutouts were prepared from 2.0 cm diameter to the maximum possible size for 15×15 applicator cone. In addition, two irregular cutouts were prepared. For each cutout, percentage depth dose (PDD) at the standard SSD and doses at different SSD values were measured using 6, 9, 12, and 16 MeV electron beam energies on a Varian 2100C LINAC and the distance at which the central axis electron fluence becomes independent of cutout size was determined. The measurements were repeated with an ELEKTA Synergy LINAC using 14×14 applicator cone and electron beam energies of 6, 9, 12, and 15 MeV. The PDD measurements were performed using a scanning system and two diodes—one for the signal and the other a stationary reference outside the tank. The doses of the circular cutouts at different SSDs were measured using PTW 0.125 cm^3 Semiflex ion-chamber and EDR2 films. The electron fluence was measured using EDR2 films.
Results: For each circular cutout, the lateral buildup ratio (LBR) was calculated from the measured PDD curve using the open applicator cone as the reference field. The effective SSD (SSD_{eff}) of each circular cutout was calculated from the measured doses at different SSD values. Using the LBR value and the radius of the circular cutout, the corresponding lateral spread parameter [$\sigma_R(z)$] was calculated. Taking the cutout size dependence of $\sigma_R(z)$ into account, the PDD curves of the irregularly shaped cutouts at the standard SSD were calculated. Using the calculated PDD curve of the irregularly shaped cutout along with the LBR and SSD_{eff} values of the circular cutouts, the output factor of the irregularly shaped cutout at extended SSD was calculated. Finally, both the calculated PDD curves and output factor values were compared with the measured values.
Conclusions: The improved LBR method has been generalized to calculate the output factor of electron therapy at extended SSD. The percentage difference between the calculated and the measured output factors of irregularly shaped cutouts in a clinical useful SSD region was within 2%. Similar results were obtained for all available electron energies of both Varian 2100C and ELEKTA Synergy machines. © *2015 American Association of Physicists in Medicine.* [http://dx.doi.org/10.1118/1.4905375]

Key words: electron beam, output, extended SSD, LBR, PDD

1. INTRODUCTION

Electron beam therapy is an integral part of treatment plans for a wide variety of tumor sites.[1–4] Most of the electron therapy treatments are performed using the nominal SSD of 100 cm. Performing electron therapy treatments at extended SSD occasionally becomes necessary, due to either anatomic restrictions or to obtain larger field sizes. Accurate and fast calculation of dosimetry from irregularly shaped cutouts at extended SSD is critical to an efficient implementation of electron therapy in the clinic. The output of simple electron beam shapes (circles, squares, rectangles, etc.) at extended SSDs has been studied by various investigators.[5–8] It has been shown that the output at extended SSD can be accurately determined using the inverse square law from an effective point source. The distance between the effective point source and the isocenter of the linear accelerator is commonly called effective SSD (SSD_{eff}). The value of SSD_{eff} depends on the energy of the electron beam, cone size, cutout size, and the type of linear accelerator. The method for SSD_{eff} determination has been described by Khan *et al.*[5] in Task Group #25 (TG-25). SSD_{eff} decreases as cutout size decreases with a more rapid decrease for smaller cutout sizes and, for a given cutout, SSD_{eff} decreases with electron beam energy. O'Shea *et al.*[9] used Monte Carlo simulation to investigate the effect of extended SSD on electron beam characteristics for different cutout sizes and electron beam energies. In the clinically relevant SSD range, the effect on the shape of the depth dose curve is insignificant.[5] In most radiation therapy clinics, the output factor values at the nominal SSD and the SSD_{eff} of simple cutout shapes are measured during commissioning of the linear accelerator. However, the output factors (OPF) of irregularly shaped cutouts at extended SSD have to be measured. In this paper, we will show that the output factor of any irregularly shaped cutout at extended SSD can be calculated by incorporating the SSD_{eff} values of circular cutouts into the improved lateral buildup ratio (LBR) method.[10]

2. MATERIAL AND METHODS

The depth dose data for this research were collected using a Varian 2100C and an ELEKTA Synergy linear accelerator equipped with a $40\times40\times40$ cm^3 water tank and PTW Dosimetry Diode E. The details of the experimental setup for the depth dose measurements are described in our previous publication.[10] The depth dose curves were measured for electron beam energies of 6, 9, 12, and 16 MeV on Varian 2100C machine and 6, 9, 12, and 15 MeV on ELEKTA Synergy machine. The data were collected using applicator of sizes of 15×15 cm^2 and 14×14 cm^2 for Varian 2100C and ELEKTA Synergy machines, respectively. Circular cutouts of diameter 2.0, 3.0, 4.0, 5.0, 6.0, 7.0, and 9.0 cm were prepared. In addition, several irregular cutouts were prepared for each machine. From the measured depth dose curves, the depth of the maximum dose (d_{max}) corresponding to each cutout and electron beam energy was determined. The diode was placed at d_{max} and the ionization charge for 100 MU was measured for SSD values of 97.5, 100.0, 105.0, 110.0, and 115.0 cm. The dose at d_{max} for each cutout, the electron beam energy, and SSD was also measured using EDR2 films. The films were irradiated with 200 MU. The optical density of the irradiated films was converted to dose using the calibration curve prepared for each electron energy.

The measured percentage depth dose (PDD) curves were normalized at the depth ($d_0 = 1.0$ mm). Figure 1 shows the normalized depth dose curves of ELEKTA Synergy using 12 MeV measured for circular cutouts of diameter 2.0, 3.0, 4.0, 5.0 cm and the open field using 15×15 cm^2 cone. Figure 2 shows the normalized depth dose curves of Varain 2100C using 12 MeV measured for circular cutouts of diameter 2.0, 3.0, 4.0, 5.0 cm and the open field using 14×14 cm^2 cone. Both figures demonstrate that, at a given depth, the dose increases with cutout size until the cutout size reaches to the minimum radius of lateral scatter equilibrium ($R_{eq} = 0.88\sqrt{E_{o,p}}$) of the electron beam. R_{eq} for electron beam energies of 6, 9, 12, and 16 MeV corresponds to 2.2, 2.6, 3.0, 3.5 cm, respectively. Further increase of the cutout size beyond R_{eq} does not significantly change the depth dose curve. The LBR at depth, z, was defined by Khan *et al.*[6] using the dose (D) and the incidence fluence of the electron field at the phantom surface (Φ) as

$$\mathrm{LBR}(R,z,E) = \frac{D(R,z,E)}{D(R_\infty,z,E)}\,\frac{\Phi_i(R_\infty,E)}{\Phi_i(R,E)}, \quad (1)$$

where R is radius of the circular cutout, R_∞ is the open field of the applicator, and E is energy of the electron beam.

It has been shown by various authors that normalizing the depth dose curves at a depth between the surface and a depth of 2–3 mm removes the dependence of the depth dose curves on the electron fluence.[6,11] For a monoenergetic electron beam

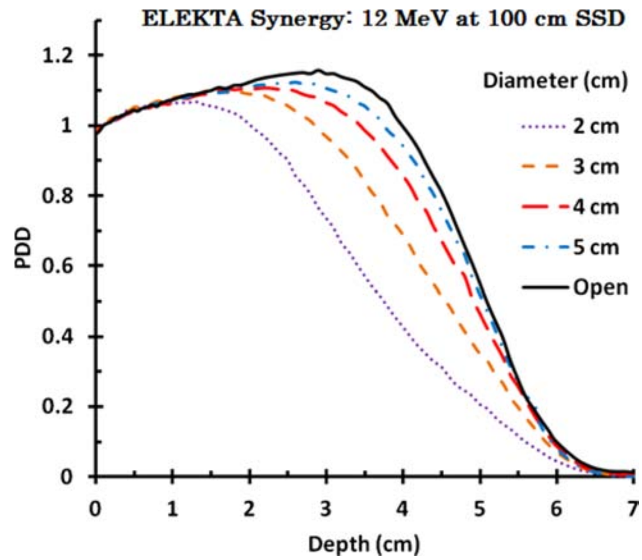

FIG. 1. Depth dose curves of ELEKTA Synergy 12 MeV for cutout diameters of 2, 3, 4, 5 cm and the open field using 15×15 cm^2 cone at SSD = 100 cm.

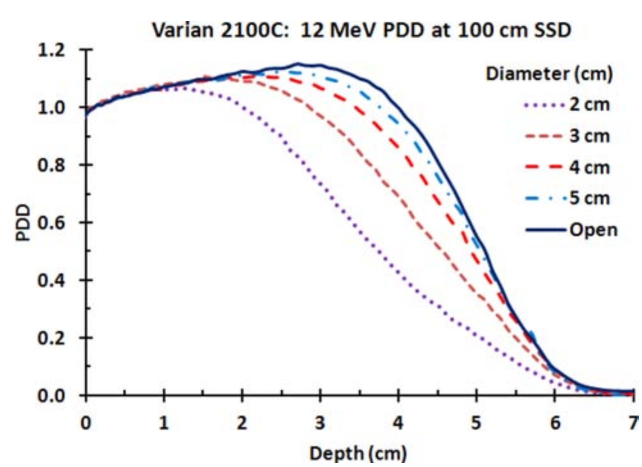

FIG. 2. Depth dose curves of Varian 2100C 12 MeV for cutout diameters of 2, 3, 4, 5 cm and the open field using 14×14 cm^2 cone at SSD = 100 cm.

incident on the surface of a homogeneous scattering medium perpendicularly, its lateral distribution as it penetrates the medium can be approximated by a Gaussian distribution. This lateral spread of the electron beam in the scattering medium is commonly represented by a lateral mean square spread parameter, $\sigma_R(z)$. At a given electron beam energy, the relation between LBR(R,z,E) and $\sigma_R(z)$ is given by[6,11]

$$\mathrm{LBR}(R,z) = 1 - \exp\left(-R^2/\sigma_R(z)^2\right). \quad (2)$$

In a clinical setup, the electrons interact with various parts of the LINAC components, including the edge of the cutout block, as they travel from the scattering foil to the surface of the medium. This causes the lateral distribution of the electron beam in the medium to lose its Gaussian shape. To account for the deviation from Gaussian shape, an empirical function of cutout size and depth dependent $\sigma_R(z)$ has been introduced *posthoc*.[10] Recently, Gebreamlak *et al.*[10] have shown that at a given z/R_p, the $\sigma_R(z)$ value increases linearly with cutout size until the cutout size reaches to the equilibrium range of the electron beam (R_{eq}). The slope of the curve is the highest near the surface and decreases as z/R_p increases. At the given z/R_p, the $\sigma_R(z)$ value for an arbitrary cutout size can be determined from the interpolation of $\sigma_R(z)$ versus cutout size curve. Chow[12] has obtained a similar result using Monte Carlo simulations.

Taking the dependence of $\sigma_R(z)$ on cutout size into account Gebreamlak *et al.*[10] calculated the depth dose distribution of an irregularly shaped field at any point P by partitioning the field into n sectors with each sector having an angle of $\Delta\theta = 2\pi/n$. Each sector of the irregularly shaped field has a unique radius and a corresponding $\sigma_R(z)$ value, which was determined from the interpolation of $\sigma_R(z)$ versus R curves. For situation where the radius crosses an edge of the cutout and then reenters the field region creating a discontinuous sector, only the first part of the sector is used in the summation. Using the sector radius and its interpolated $\sigma_R(z)$ value, the corresponding LBR(R,z) value was determined. Finally, the dose per MU, $D_0(u,z)$, for the irregularly shaped cutout, u, at the standard SSD can be calculated using the equation[6]

$$D_0(u,z) = K_0 \frac{\mathrm{PDD}_0(R_0,z)}{100} J_0(R_c) \frac{\Delta\theta}{2\pi} \times \sum_{i=1}^{n} \left[\mathrm{LBR}_0(R_{i,c},z) \times I_0(R_{i,c})\right], \quad (3)$$

where K_0 is the dose/MU for a broad field reference applicator of size R_0 at the depth z_m of the dose maximum for the broad field; PDD$_0(R_0,z)$ is the relative depth dose curve of the broad field, normalized to the dose at z_m; $J_0(R_c)$ is the applicator factor which is equal to the incident fluence for the given applicator of size R_c relative to the reference applicator of size R_0; $I_0(R_{i,c})$ is the insert factor which is equal to the incident fluence factor for insert of radius $R_{i,c}$ in an applicator of size R_c relative to the open applicator. In this research, the normalization depth (d_0) is chosen to be between 0.5 and 1.0 mm. $J_0(R_c)$ is constant for a given cutout and beam energy. For absolute dose distribution, its value can be determined using film or diode. However, it has no effect on the normalized depth dose distribution and is absorbed in the normalization.

3. DATA ANALYSIS

Figure 3 shows the schematic diagrams of "S" and U shaped cutouts using ELEKTA Synergy and Varian 2100C, respectively. Figures 4 and 5 compare the calculated PDD curves using the "interpolated $\sigma_R(z)$" method with the measured PDD curves for the S and U shaped cutouts for four electron beam energies, respectively. In the region between the surface and $z/R_p = 0.6$, which contains the clinically useful depth, the percentage difference between the measured and calculated values of both cutouts for each electron beam energy was within 2%.

The dose per MU, $D_g(u,z)$, for an irregularly shaped cutout at extended SSD of gap g can be determined by replacing all the parameters of Eq. (3) by their corresponding values at

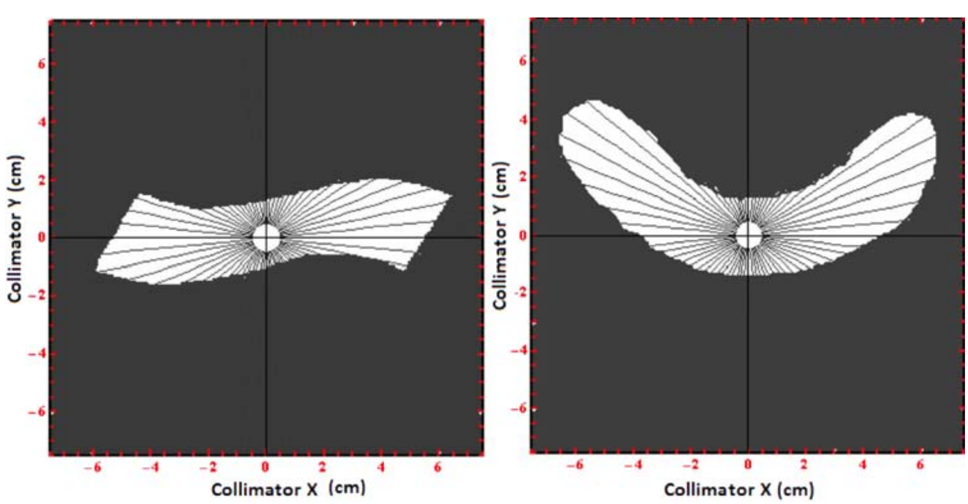

FIG. 3. The schematic diagrams of the S (lefthand figure) and U shaped (righthand figure) cutouts prepared using ELEKTA Synergy 14 × 14 cm^2 cone and Varian 2100C 15 × 15 cm^2 cone, respectively. Each cutout is divided into 64 sectors with each sector having an angle of $\pi/32$ rad. The depth dose curves and output factors of the cutouts are measured at the intersection of the sectors.

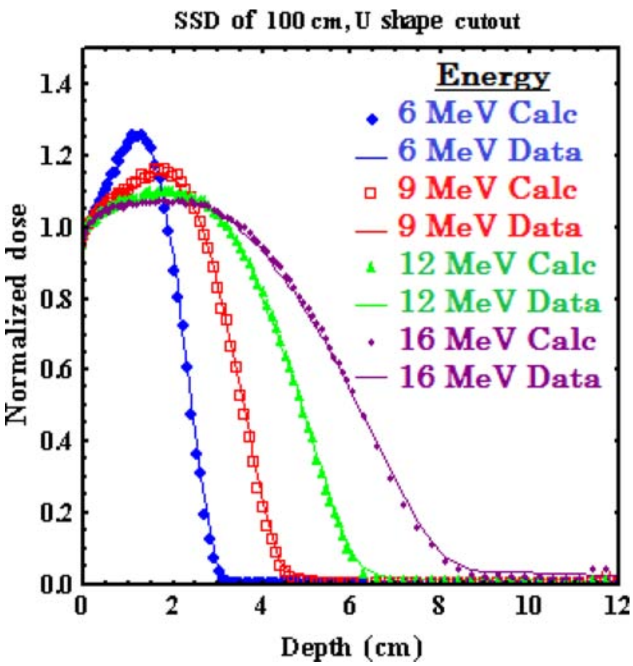

FIG. 4. Comparison of the measured (Data) and the calculated (Calc) depth dose curves, normalized at $d_0 = 1$ mm, of the "U" shaped cutout for Varian 2100C electron beam energies of 6 MeV (diamond), 9 MeV (open square), 12 MeV (triangle), and 16 MeV (circle) at SSD = 100 cm.

extended SSD. Thus, $D_g(u,z)$ takes the form

$$D_g(u,z) = K_g \frac{\mathrm{PDD}_g(R_0,z)}{100} J_g(R_c) \frac{\Delta\theta}{2\pi} \times \sum_{i=1}^{n} \left[\mathrm{LBR}_g(R_{i,c},z) \times I_g(R_{i,c})\right]. \tag{4}$$

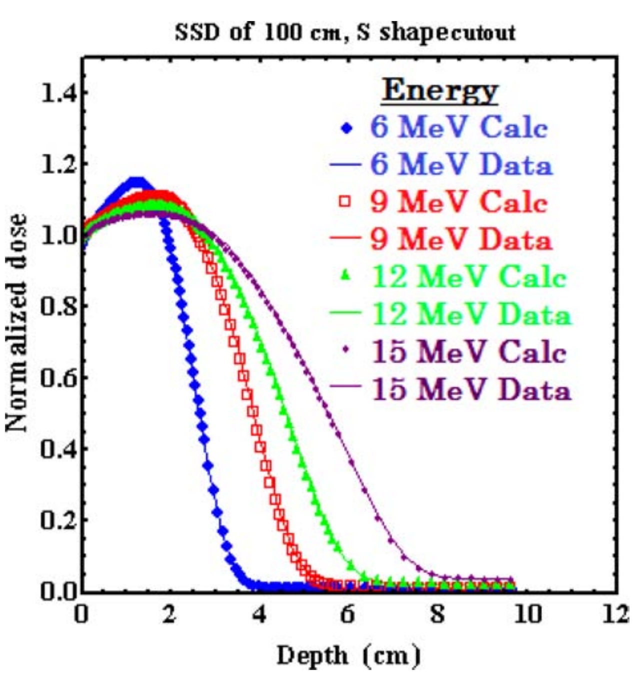

FIG. 5. Comparison of the measured (Data) and the calculated (Calc) depth dose curves, normalized at $d_0 = 1$ mm, of the S shaped cutout for ELEKTA Synergy electron beam energies of 6 MeV (diamond), 9 MeV (open square), 12 MeV (triangle), and 15 MeV (circle) at SSD = 100 cm.

The central axis depth doses of a cutout at gap distance g and at the standard SSD ($g = 0$) are related by the equation[13]

$$D_g(R,z) = D_0(R,z) * \mathrm{SF}_g(R,z), \tag{5}$$

where $D_0(R,z)$ is depth dose of the cutout at depth z and standard SSD, $D_g(R,z)$ is the depth dose of the cutout at depth z and gap distance g, and $\mathrm{SF}_g(R,z)$ is the gap factor of the cutout. The gap factor of the cutout is used solely to determine the output at the maximum of the field and can be determined from the relation[5]

$$\mathrm{SF}_g(R,z) = \left[\frac{\mathrm{SSD}_{\mathrm{eff}}(R)+z}{\mathrm{SSD}_{\mathrm{eff}}(R)+z+g}\right]^2, \tag{6}$$

where $\mathrm{SSD}_{\mathrm{eff}}$ is the effective SSD of the cutout to the standard SSD. Figure 6 shows the relation between $\mathrm{SSD}_{\mathrm{eff}}$ and circular cutout radius for Varian 2100C machine using electron beam energies of 6, 9, 12, and 16 MeV. The relation between parameters of Eqs. (4) and (3) can be established using the above gap factor term as

$$K_g = K_0 * \mathrm{SF}_g(R_0,d_{\max}), \tag{7}$$

$$J_g(R_c) = J_0(R_c)\frac{\mathrm{SF}_g(R_c,d_0)}{\mathrm{SF}_g(R_0,d_0)}, \tag{8}$$

$$I_g(R_{i,c}) = I_0(R_{i,c})\frac{\mathrm{SF}_g(R_{i,c},d_0)}{\mathrm{SF}_g(R_c,d_0)}, \tag{9}$$

$$\mathrm{PDD}_g(R_0,z) = \mathrm{PDD}_0(R_0,z)\frac{\mathrm{SF}_g(R_0,z)}{\mathrm{SF}_g(R_0,d_{\max})}, \tag{10}$$

$$\mathrm{LBR}_g(R_{i,c},z) = \mathrm{LBR}_0(R_{i,c},z)\frac{\mathrm{SF}_g(R_{i,c},z)}{\mathrm{SF}_g(R_0,z)}\frac{\mathrm{SF}_g(R_0,d_0)}{\mathrm{SF}_g(R_{i,c},d_0)}. \tag{11}$$

Substituting Eqs. (7)–(11) into Eq. (4) and simplifying the resulting expression gives

$$D_g(u,z) = K_0 \frac{\mathrm{PDD}_0(R_0,z)}{100} J_0(R_c) \frac{\Delta\theta}{2\pi} \times \sum_{i=1}^{n} \left[\mathrm{LBR}_0(R_{i,c},z) I_0(R_{i,c}) \mathrm{SF}_g(R_{i,c},z)\right]. \tag{12}$$

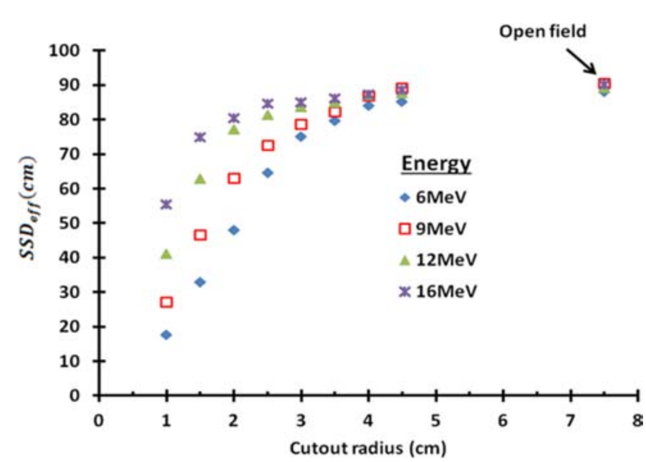

FIG. 6. Plots of $\mathrm{SSD}_{\mathrm{eff}}$ (cm) versus circular cutout radius (cm) of Varian 2100C machine for electron energies of 6, 9, 12, 16 MeV.

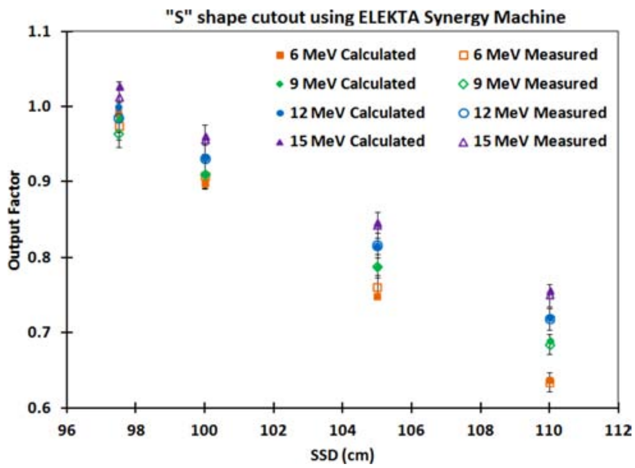

FIG. 7. Comparison of the measured and the calculated OPF values of the ELEKTA Synergy machine for the S shaped cutout as a function of SSD (cm) for electron beam energies of 6, 9, 12, and 15 MeV. Error bar of size 2% is added to the measured output factor values.

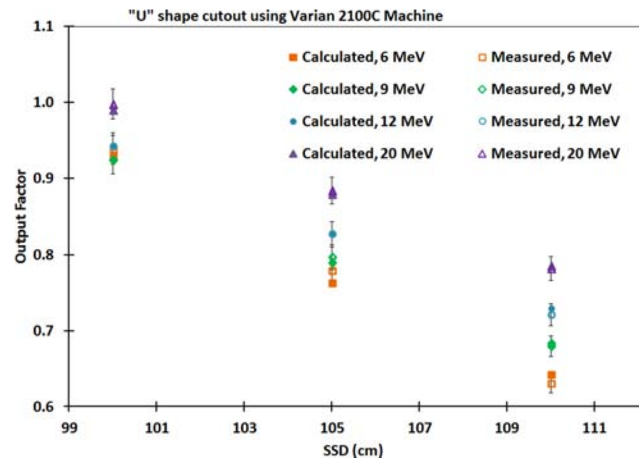

FIG. 8. Comparison of the measured and the calculated OPF values of the Varian 2100C machine for the U shaped cutout as a function of SSD (cm) for electron beam energies of 6, 9, 12, and 20 MeV. Error bar of size 2% is added to the measured output factor values.

The output factor, $\mathrm{OPF}_g(u)$, of the irregular cutout at extended SSD is the ratio of the maximum dose of the irregular cutout at the extended SSD, $[D_g(u)]_{\max}$, to the maximum dose of the reference field at the standard SSD, $[D_0(R_0)]_{\max}$. Mathematically, it is given by

$$\mathrm{OPF}_g(u) = \frac{[D_g(u)]_{\max}}{[D_0(R_0)]_{\max}}. \tag{13}$$

In general, the electron fluence along the central axis of the electron beam varies with cutout sizes mainly due to different levels of blocking and scattering from the edge of the cutouts. This variation of electron fluence between cutouts sides, however, decreases as the distance between the cone and the surface of the phantom decreases and at some distance, $|g_0|$, $I_{g_0}(R_{ic})$ becomes equal to one. This distance was determined using both film and diodes with good agreement between the two methods. Note that g_0 is negative since it is above the position of the standard SSD. If the maximum dose values of the irregular cutout and the reference field at g_0 are $[D_{g_0}(u)]_{\max}$ and $[D_{g_0}(R_0)]_{\max}$, respectively, then Eq. (13) can be rewritten as

$$\mathrm{OPF}_g(u) = \mathrm{SF}_{g_0}(R_0)\left(\frac{[D_{g_0}(u)]_{\max}}{[D_{g_0}(R_0)]_{\max}}\right)\left(\frac{[D_g(u)]_{\max}}{[D_{g_0}(u)]_{\max}}\right). \tag{14}$$

The leftmost term is the gap factor of the reference field at position g_0. From our diode and EDR2 film measurements, the values of g_0 for the Varian 2100C and the ELEKTA Synergy machines were close to −4.0 and −1.5 cm, respectively. Since g_0 is negative, the gap factor is greater than one. The middle term is the ratio of the maximum dose of the irregular cutout to the maximum dose of the reference field at position g_0. Since the electron fluence along the central axis at this position is the same for all cutouts, the ratio can be determined by first normalizing the depth dose curves of both the irregular cutout and the reference field at the normalization depth and then calculating the ratio of their maximum values. The rightmost term can be determined from Eq. (12) as

$$\frac{[D_g(u)]_{\max}}{[D_{g_0}(u)]_{\max}} = \frac{\left[\mathrm{PDD}_0(R_0,z)\sum_{i=1}^{n}\left[\mathrm{LBR}_0(R_{i,c},z)\frac{\mathrm{SF}_g(R_{i,c},z)}{\mathrm{SF}_{g_0}(R_{i,c},d_0)}\right]\right]_{\max}}{\left[\mathrm{PDD}_0(R_0,z)\sum_{i=1}^{n}\left[\mathrm{LBR}_0(R_{i,c},z)\frac{\mathrm{SF}_{g_0}(R_{i,c},z)}{\mathrm{SF}_{g_0}(R_{i,c},d_0)}\right]\right]_{\max}}. \tag{15}$$

4. RESULTS AND DISCUSSION

Figure 7 compares the calculated output factor using Eq. (14) for the S shaped irregular cutout as a function of g with the measured output factor values for ELEKTA Synergy machine electron beam energies of 6, 9, 12, and 15 MeV, respectively, with 2% error bars added to the measured output factor values. Figure 8 compares the calculated output factor the U shaped irregular cutout as function of g with the measured output factor values for Varian 2100C machine electron beam energies of 6, 9, 12, and 20 MeV, respectively, with 2% error bars added to the measured output factor values. In all cases, the percentage differences between the measured and the calculated output factor values were within 2%. The measured output factors of four irregular patient cutouts for different SSD values and energies were compared with the output factors obtained using our proposed method. The percentage differences were within 2%.

5. CONCLUSION

The output factor of irregularly shaped electron cutouts at standard and at extended SSD values is determined by measurements. This is labor and time consuming. In addition, it is exposed to human error. In this paper, we have shown that the output factor of any irregularly shaped cutout at extended SSD can be calculated using $\mathrm{SSD}_{\mathrm{eff}}$ values of circular cutouts and their PDD curves measured at standard SSD. The percentage difference of the calculated output factors from the measured values in a clinically useful SSD region for both ELEKTA Synergy and Varian 2100C machines was within 2%.

ACKNOWLEDGMENT

The authors thank South Carolina Oncology Associates (SCOA) for access to materials and machine time.

[a]Author to whom correspondence should be addressed. Electronic mail: wondtassew@gmail.com

[1]K. R. Hogstrom and P. R. Almond, "Review of electron beam therapy physics," Phys. Med. Biol. **51**, R455–R489 (2006).

[2]N. D. Tapley, *Clinical Applications of the Electrons Beam* (Wiley, New York, NY, 1976).

[3]K. R. Hogstrom, R. A. Boyd, J. A. Antolak, M. M. Svatos, B. A. Faddegon, and J. G. Rosenman, "Dosimetry of a prototype retractable emlc for fixed-beam electron therapy," Med. Phys. **31**, 443–460 (2004).

[4]K. K. Wooden, K. R. Hogstrom, P. Blum, R. J. Gastorf, and J. D. Cox, "Whole-limb irradiation of the lower calf using a six-field electron technique," Med. Dosim. **21**, 211–218 (1996).

[5]F. M. Khan, K. P. Doppke, K. R. Hostrom, G. J. Kutcher, R. Nath, S. C. Prasad, J. A. Purdy, M. Rozenfeld, and B. L. Werner, "Clinical electron-beam dosimetry," Med. Phys. **18**, 73–109 (1991).

[6]F. M. Khan, P. D. Higgins, B. J. Gerbi, F. C. Deibel, A. Sethi, and D. N. Mihailidis, "Calculation of depth dose and dose per monitor unit for irregularly shaped electron fields," Phys. Med. Biol. **43**, 2741–2754 (1998).

[7]K. R. Hogstrom, M. D. Mills, and P. R. Almond, Phys. Med. Biol. **26**, 445–459 (1981).

[8]F. F. Khan, *The Physics of Radiation Therapy*, 4th ed. (Williams and Wilkins, Baltimore, Maryland, 2010).

[9]T. P. O'Shea, M. J. Foley, D. Rajasekar, P. A. Downes, W. van Putten, M. Moore, and A. Shearer, "Electron beam therapy at extended source-to-surface distance: A Monte Carlo inverstigation," J. Appl. Clin. Med. Phys. **9**, 57–67 (2008).

[10]W. T. Gebreamlak, D. J. Tedeschi, and H. A. Alkhatib, "Dose calculation for electron therapy using an improved LBR method," Med. Phys. **40**, 071717 (7pp.) (2013).

[11]E. Tyner, P. McCavana, and B. McClean, "A modified method of calculating the lateral build-up ratio for small electron fields," Phys. Med. Biol. **51**, N241–N246 (2006).

[12]J. C. L. Chow, "Calculation of lateral buildup ratio using Monte Carlo simulation for electron radiotherapy," Med. Phys. **34**, 175–182 (2007).

[13]D. M. Roback, F. M. Khan, J. P. Gibbsons, and A. Sethi, "Effective SSD for electron beams as a function of energy and beam collimation," Med. Phys. **22**, 2093–2095 (1995).